

Heat capacity measurement of molten $\text{NaNO}_3\text{-NaNO}_2\text{-KNO}_3$ by drop calorimetry

M. KAWAKAMI, K. SUZUKI, S. YOKOYAMA, and T. TAKENAKA

Department of Production Systems Engineering, Toyohashi University of Technology, Japan

Molten $\text{NaNO}_3\text{-NaNO}_2\text{-KNO}_3$ mixture is used as a heat transfer medium at high temperature. One of the most important properties of this mixture is the heat capacity. In the present work, the enthalpy change with temperature was measured by the drop calorimetric method to evaluate the heat capacity. The results are summarized as follows:

The enthalpy of the mixture increased linearly with the temperature. From the slope of the line, the heat capacity was evaluated. The heat capacity of pure NaNO_3 , NaNO_2 and KNO_3 was 0.129, 0.110 and 0.142 kJ/mol/K, respectively. These values are in fairly good agreement with the published data. In the binary and ternary systems, the molar additivity of heat capacity, which is well known as Neumann-Kopp's law, was obtained. The heat capacity of HTS_1 and HTS_2 , which are well known ternary mixtures of practical use, were in the range of published data.

Introduction

The HTS_1 (7 mass per cent NaNO_3 -40 mass per cent NaNO_2 -53 mass per cent KNO_3) and HTS_2 (50 mole per cent NaNO_3 -50 mole per cent KNO_3) are used as a heat transfer medium at high temperature such as in a petroleum refinery¹. One of the most important physical properties is the heat capacity of the heat transfer medium. Although the heat capacity data of constituent single salt were published²⁻¹¹, those of the mixture were very poor^{1,5,12-14}. The heat capacity has been measured by drop calorimetric methods in which some kind of capsule like a platinum capsule was used¹¹. But the capsulation process is complicated and leads to some errors. In the present work, the heat capacity was measured in a wide composition range of $\text{NaNO}_3\text{-NaNO}_2\text{-KNO}_3$ system by the simplified drop calorimetric method in which the molten salt sample was directly dropped in to the calorimeter.

Experimental method

Chemical reagent

The used reagents of NaNO_3 , NaNO_2 and KNO_3 were of the best grade. These reagents are wettable. They have been dehydrated by keeping them at about 393 K in the evacuated chamber for ten hours^{2,5,8,9}. In the present work, it was found that the weight became constant after keeping at 402 K in ambient atmosphere for 24 hours. In practice, the reagents were kept at 405 K for more than 24 hours before use. The reagents were weighed with the accuracy of 0.1 mg and mixed to the desired composition just before the measurement. The composition is shown in Figure 1.

In the binary system, the composition was 20 mole per cent plus HTS_2 (50 mole per cent NaNO_3 -50 mole per cent KNO_3). In the ternary system, the composition was selected on the connecting line of pure NaNO_3 and HTS_1 .

Apparatus

Figure 2 shows the experimental apparatus.

The calorimeter was composed of Dewar vessel, stirrer, plastic lid and thermistor tip. The Dewar vessel was of 100 mm inner diameter, 155 mm depth, and made of stainless steel. The stirrer was the impeller with a plastic blade of 10 mm \times 20 mm and driven by the outside motor at 1 200 rpm. The plastic lid was made of foamed plastics and with a silica tube of 20 mm inner diameter through which the molten salt was dropped. The thermistor tip was used to measure the temperature of water in the vessel with good accuracy in a short temperature range. The tip was connected to the electric bridge circuit. The output of the circuit was calibrated with the Beckmann thermometer with 0.01 degree accuracy.

The salt melting unit was put on the calorimeter. It was composed of heating furnace, Tammann tube and stopper rode. The furnace was a resistance heating one of 30 mm inner diameter, 60 mm outer diameter, and 120 mm length. The Tammann tube was made of mullite and of 20 mm inner diameter and 120 mm length. The stopper of 36 mm

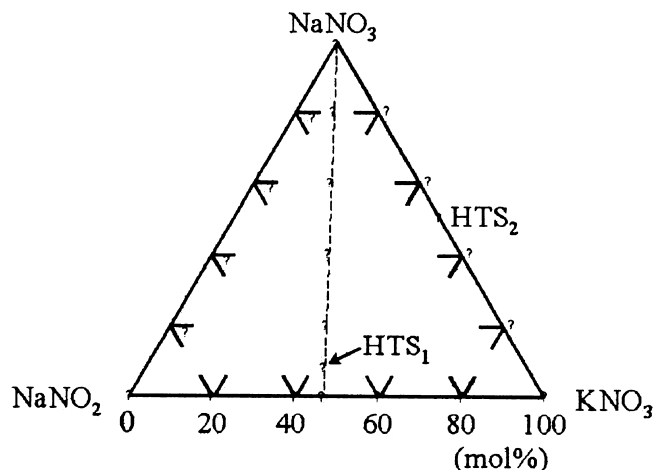


Figure 1. Experimental composition of salt on ternary diagram

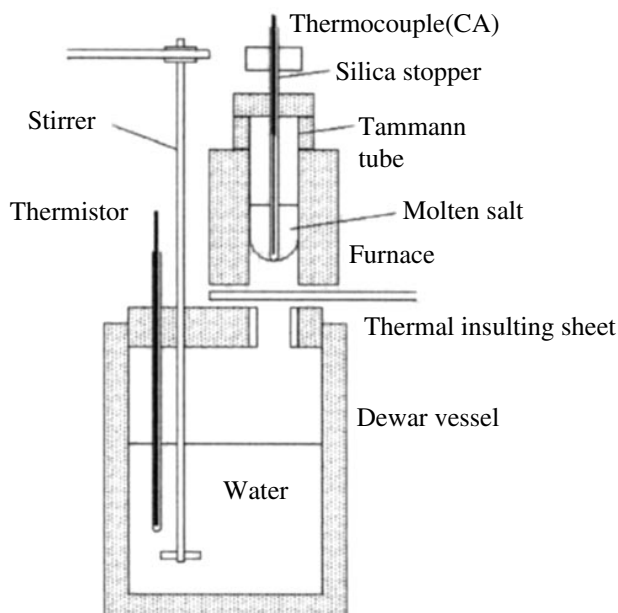


Figure 2. Schematic diagram of experimental apparatus

outer diameter was fixed to the top of the tube by alumina cement in order to keep the molten salt at the isothermal zone of the furnace. On the bottom of tube, a small hole of 4 mm ϕ was opened. The hole was closed by the silica tube of 6.3 mm outer diameter with one closed end. The Almel-Chromel thermocouple was inserted in the silica tube to measure the temperature of the molten salt.

The following procedure was adopted in order to obtain precisely 500.0 g of water in the Dewar vessel. At first, the distilled water was put into the measuring cylinder to the level of 500 ml. The weight was measured to the precision of 0.1 g. by the balance. The distilled water was poured into the Dewar vessel. The weight of the empty cylinder was measured again. From the difference between the two weights, the weight of poured water was obtained. The additional distilled water was supplied to the vessel with the measuring pipette up to 500.0 g precisely.

Setting up of the apparatus

The calorimeter was set on the bottom of the framework. The furnace was fixed to the framework just above the calorimeter. The Tammann tube was fixed to the furnace, so that the centre of bottom hole of the tube would be on the central axis of the silica tube of the calorimeter. The bottom hole of the Tammann tube was closed tightly with the silica tube. The silica tube was fixed by the weight which was attached to the top of it. The thermocouple was inserted in to the silica tube. The thermal insulating sheet of stainless steel was inserted in the space between the calorimeter and the furnace.

Procedure

The weight of the Tammann tube and silica stopper tube was measured before setting up by the electronic balance with the accuracy of 0.1 mg. The composition of the sample was adjusted by the preceding method. The sample weight was determined to 10.000 g by the preliminary measurement, so that the temperature change of calorimeter should be 2 to 4 degrees. The sample was inserted in the Tammann tube on which the ceramic fibre was put for

thermal insulation. The furnace was heated to 650 K at first to confirm the complete melting of the sample mixture. Then, the temperature of the sample was adjusted to the desired one, kept for some time and stirred with a thin steel rod. After confirming the constant temperature of the sample, the stirrer of the calorimeter was switched on. After confirming the constant temperature rise in the calorimeter, the thermal insulating sheet between the calorimeter and the furnace was removed and the sample was dropped in the calorimeter. After the dropping, the thermal insulating sheet was inserted again. The temperature change was monitored until a temperature rise of the same rate as before the sample dropping was obtained. After the measurement, the Tamman tube and silica stopper tube were taken out from the furnace and their weight was measured with an accuracy of 0.1 mg. Comparing their weight before and after the measurement, the residual weight of salt was estimated and subtracted from the initial sample weight to obtain the weight of the dropped sample with an accuracy of 1 mg.

Data processing

Figure 3 shows an example of the recorded chart of the thermistor circuit output.

The temperature of the calorimeter increased at a constant rate before the sample dropping. At the sample dropping, the temperature jumped up suddenly and increased gradually and finally at the same constant rate as that before the sample dropping. Extrapolating the curve down to the moment at which the sample dropped, the temperature increase, namely $T_2 - T_1$, by the sample drop was estimated. The heat absorbed by the calorimeter Q_c was given by

$$Q_c = W_o(T_2 - T_1) \quad [1]$$

Where, W_o is the water equivalent of the calorimeter. This heat should be liberated from the salt sample during the change from molten state at temperature T to dissolved state in water at T_2 . Therefore,

$$H_T - H_{T_2}(aq.) = Q_c M / W \quad [2]$$

Where M is the formula weight of the salt sample and W is the weight of sample. The formula of the mixture was given by

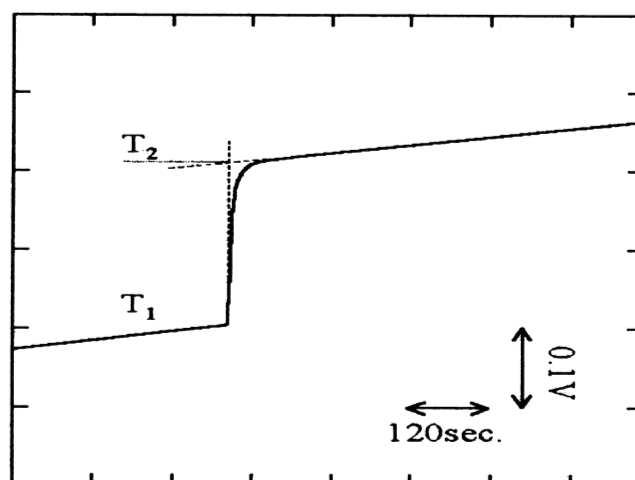


Figure 3. An example of recorder output from the thermistor circuit in the calorimeter

$$M = \sum M_i X_i \quad [3]$$

Where, M_i is the formula weight of pure salt 'i' and X_i in the mole fraction of 'i' in the system.

Figure 4 shows the schematic diagram of $H_T - H_{T2}(aq.)$ as a function of temperature.

It is seen from the figure that the $H_T - H_{T2}(aq.)$ includes the heat of dissolution to water $\Delta H_{sol.}$. In order to obtain the standard enthalpy change, the heat of dissolution and $H_{T2} - H_{298}$, which is the enthalpy change of solid phase, should be evaluated and corrected. Namely,

$$H_T - H_{298} = H_T - H_{T2}(aq.) - \Delta H_{sol.} + H_{T2} - H_{298} \quad [4]$$

Determination of water equivalent and

The water equivalent of the calorimeter was determined using the pure copper piece which was a cylinder with cone head in shape. This piece was heated in the alumina crucible of 43 mm inner diameter and 37 mm depth using a resistance furnace other than that shown in Figure 2. After reaching constant temperature, the crucible was taken out of the furnace and brought to the calorimeter. The copper piece was taken out and was thrown into the calorimeter. The temperature change of calorimeter ΔT_c was obtained in the same way as above. Then, the water equivalent was obtained by

$$W_o = Q_s / \Delta T_c \quad [5]$$

Where Q_s is the heat brought by the copper piece to the calorimeter and given by

$$Q_s = w_s c_{ps} dT - Q_{loss} \quad [6]$$

Where c_{ps} is the heat capacity of copper, w_s is the mass of copper piece and Q_{loss} is the heat loss during transfer to the calorimeter.

Determination of enthalpy change of the solid phase

The solid piece with the respective composition was made by the following method. The reagents were weighed and mixed to the desired composition. The mixture was melted at 650 K, cast into the mould and solidified in the desiccator. The solidified piece was cylindrical and of 16 mm ϕ and 30 mm length. The solid piece was put into the same alumina crucible as above. The total weight of the solid piece and crucible was measured with an accuracy of

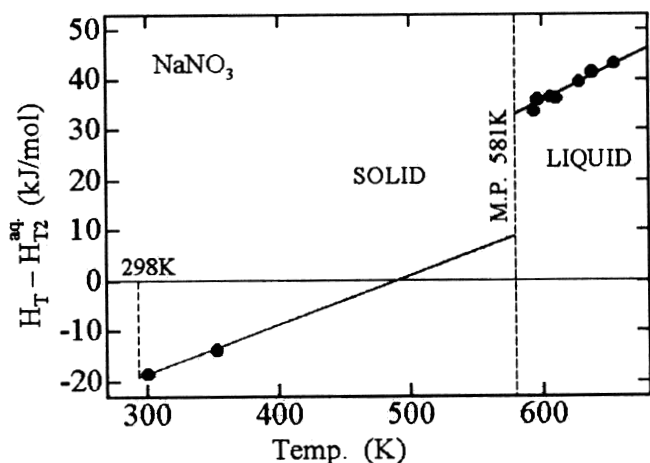


Figure 4. An example of enthalpy change with temperature

0.1 mg. The crucible with the solid piece was heated in the same furnace as used in the determination of water equivalent. After reaching the constant temperature, the solid piece was taken out and thrown into the calorimeter in the same way as above. After the piece dropped, the total weight of the crucible and residual solid piece was measured again. The difference between the weights before and after the experiment gave the weight of the solid piece thrown into the calorimeter. The enthalpy change of the solid phase was estimated in the same way as in the case of the liquid phase. The temperature range was 290 to 315 K.

Result and discussions

Water equivalent

Two kinds of copper piece were used. One piece was of 47.428 g and the other 135.214 g. The temperature before dropping into the calorimeter was 372 to 422 K. The heat capacity data of pure copper were expressed as a linear function of temperature using the data of 0.383 J/gK at 293 K and 0.398 J/gK at 373 K¹⁵ and used for the calculation of Equation [6]. The value of Q_{loss} was about 0.2 per cent as will be explained later. The corrected data of the water equivalent are shown in Table I. Taking the total average, the water equivalent was determined as 2.199 kJ/K.

Heat of dissolution and enthalpy of the solid phase

Assuming that the enthalpy of the solid phase should be expressed by the linear function of temperature, the enthalpy change was plotted against $T = 298 + T_s - T_2$, where T_s is the temperature of the solid piece before dropping. The enthalpy change at 298 K should be the dissolution heat of salt into water. Then the subtraction of the dissolution heat from the enthalpy change will give the standard enthalpy of the solid phase, $H_T - H_{298}$. The heat of dissolution and $H_T - H_{298}$ are summarized in Table II.

The literature data for heat of dissolution were -20.50 kJ/mol for NaNO_3 , -13.89 kJ/mol for NaNO_2 , and -34.9 kJ/mol for KNO_3 ¹⁵. The results of the present work were in fairly good accordance with them. The value of a in Table II can be considered as the heat capacity of the solid phase. The literature data for heat capacity for pure salts, HTS_1 and HTS_2 are compared with the present results in Table III.

Table I
Water equivalent of calorimeter

Piece Weight, g	Temperature, K	Water Eq. kJ/K
47.428	374.03	2.202
	381.64	2.198
	381.25	2.198
	379.67	2.197
	378.93	2.196
	380.76	2.202
	379.45	2.203
135.214	416.11	2.205
	422.22	2.195
	408.16	2.200
	390.31	2.198
	387.13	2.198
	383.83	2.203
	376.57	2.194
	372.16	2.200
	375.79	2.196
	376.07	2.202

Table II
Heat of dissolution into water and enthalpy of solid phase

Composition, mol%			DH _{sol.} kJ/mol	HT-H ₂₉₈ =
NaNO ₃	NaNO ₂	KNO ₃		aT-b
100	0	0	-20.971 (-20.50)	0.123
0	100	0	-14.478 (-13.89)	0.123
0	0	100	-35.653 (-34.9)	0.131
20.00	80.00	0.00	-15.361	0.119
40.00	60.00	0.00	-16.327	0.126
60.00	40.00	0.00	-16.822	0.114
80.00	20.00	0.00	-18.163	0.141
0.00	20.00	80.00	-30.703	0.112
0.00	40.00	60.00	-26.571	0.119
0.00	60.00	40.00	-22.569	0.118
0.00	80.00	20.00	-18.651	0.078
80.00	0.00	20.00	-23.479	0.112
60.00	0.00	40.00	-26.207	0.102
50.00	0.00	50.00	-27.420	0.143
40.00	0.00	60.00	-29.036	0.103
20.00	0.00	80.00	-32.372	0.137
6.94	48.87	44.19	-23.984	0.101
0.00	52.50	47.50	-24.540	0.126
20.00	42.00	38.00	-23.015	0.102
40.00	31.50	28.50	-21.576	0.132
60.00	21.00	19.00	-22.010	0.128
80.00	10.50	9.50	-20.361	0.131

The values in parentheses are from literature¹⁵

Table III
Heat capacity of solid phase

	c _p (s), J/K/mol	
	Present work	Literature
NaNO ₃	123	92 ²⁾ , 13 ¹⁶⁾
NaNO ₂	123	133 ⁸⁾
KNO ₃	131	95 ²⁾ , 132 ⁹⁾
HTS ₁	101	113 ¹⁾
HTS ₂	143	127 ⁶⁾ , 132 ¹³⁾

For NaNO₃ and KNO₃, the present result was within the published data. For NaNO₂, the present result was slightly smaller than that of Cases⁸. The present result for HTS₁ was slightly smaller than that of Kirst *et al.*¹. On the contrary, the present result for HTS₂ was slightly larger than the literature data. Although there were some differences, they were not so large. Therefore, the heat of dissolution and heat capacity of the solid phase shown here were used to estimate the standard enthalpy of the liquid phase.

The standard enthalpy of the liquid phase

Figure 5 shows the standard enthalpy of pure salts.

It changed linearly with temperature, showing the constant heat capacity within the experimental temperature range. The standard enthalpy of NaNO₃ was the largest among them. That of KNO₃ was the second and that of

NaNO₂ was the smallest. Their temperature dependency was given by

For NaNO₃,

$$H_T - H_{298} = 0.129(\pm 0.003)T - 21.321(\pm 1.517) \text{ kJ/mol} \quad [7]$$

For NaNO₂,

$$H_T - H_{298} = 0.110(\pm 0.003)T - 13.267(\pm 1.883) \text{ kJ/mol} \quad [8]$$

For KNO₃,

$$H_T - H_{298} = 0.142(\pm 0.005)T - 32.149(\pm 3.086) \text{ kJ/mol} \quad [9]$$

The figures in parentheses show the standard deviation of the least squares method

Figure 6 shows the standard enthalpy of the NaNO₃-NaNO₂ binary system.

The data of each composition seemed to coincide with each other except for 80 mole percent NaNO₃ where the data was the largest. The data can be expressed by the linear function of temperature. It can be seen that the slope

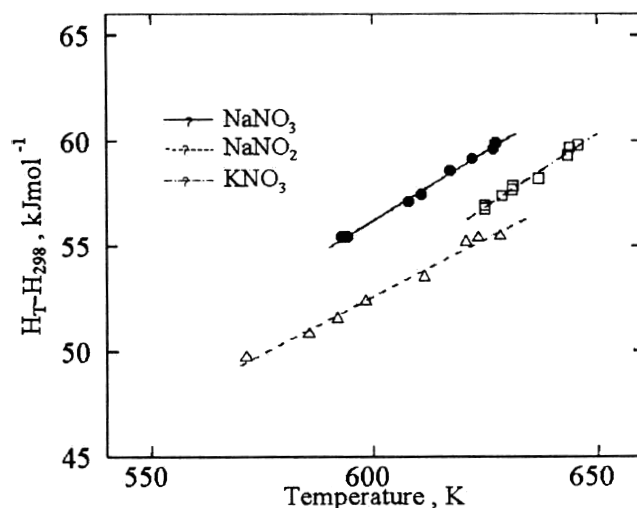


Figure 5. Standard enthalpy of pure liquid salts

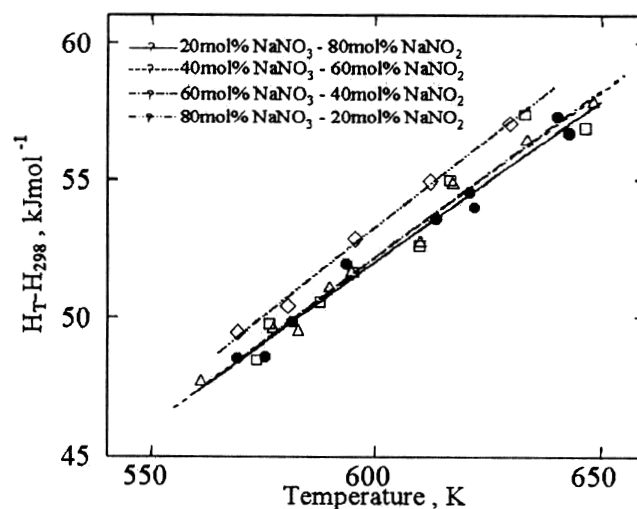


Figure 6. Standard enthalpy of liquid NaNO₃-NaNO₂ system

increased with the mole per cent of NaNO_3 in this system. Figure 7 shows the standard enthalpy of the NaNO_2 - KNO_3 binary system.

In this system, the data of each composition seemed also to coincide with each other. The linearity of the data seemed better than that in the NaNO_3 - NaNO_2 system. The slope increased clearly with the mole per cent of KNO_3 . Figure 8 shows the standard enthalpy of the KNO_3 - NaNO_3 binary system.

The enthalpy increased linearly with temperature as the other systems. Although the absolute value increased with NaNO_3 content, the slope of the line did not seem to change so much.

Heat capacity of the liquid phase

The heat capacity can be obtained by differentiating the standard enthalpy from the absolute temperature. As shown above, all the data of the standard enthalpy in the present work had a linear relation with the temperature. Therefore, the slope of the lines shown in Figures 6 to 8 gives the heat capacity. Table IV shows the heat capacity of pure salts, HTS_1 and HTS_2 .

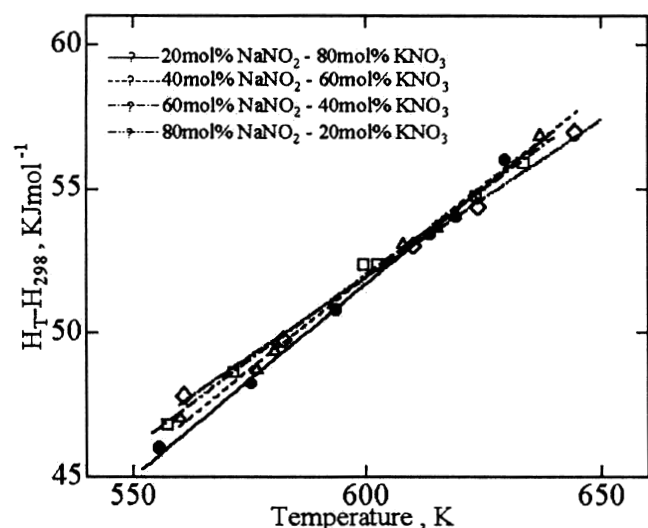


Figure 7. Standard enthalpy of liquid NaNO_2 - KNO_3 system

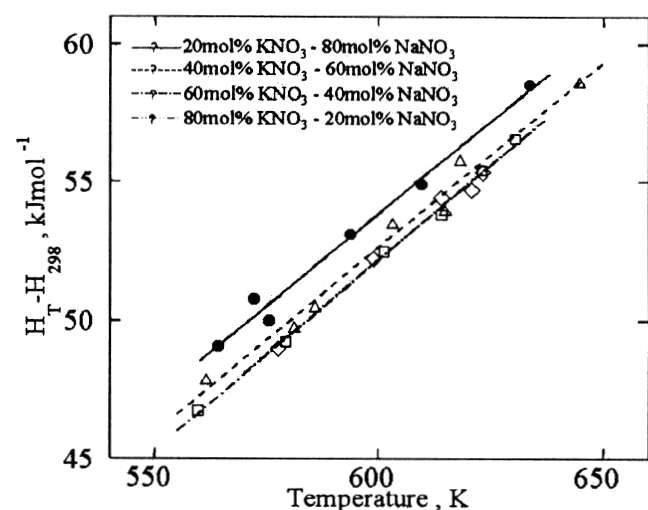


Figure 8. Standard enthalpy of liquid KNO_3 - NaNO_3 system

Table IV also shows the literature data for the respective materials. The present data were smaller than the published data for NaNO_3 . Although the published data scattered from 100 to 120 J/K/mol, the present data were in the middle of them for NaNO_2 . The published data were mostly around 140 J/K/mol for KNO_3 . The present data accorded well with them. Although the published data were 131 and 132 J/K/mol for HTS_1 , the present result was slightly smaller. The literature data for HTS_2 scattered widely from 136 to 155 J/K/mol. The present result was just in the middle of them. All the other binary and ternary data obtained in the present work are summarized in Table V.

In Table V, the liquidus temperature is also shown. It was determined by thermo-analysis for the respective compositions. Figure 9 shows the change of heat capacity with composition in NaNO_3 - NaNO_2 and KNO_3 - NaNO_3 systems.

In both systems, the data of the mixture lie on the straight line connecting those of the pure constituents. This is called the Neumann-Kopp's law in which the heat capacity of the mixture should be the sum of the heat capacities of the constituent elements. Figure 10 shows the change of heat capacity with composition in the NaNO_2 - KNO_3 system.

Neumann-Kopp's law can also be seen in this binary system. In Figure 10, the data by Iwadata *et al.*⁷ were shown. They are in good accordance with the present results.

Table IV
Heat capacity of liquid phase

	$c_p(s)$, J/K/mol	
	present work	literature
NaNO_3	129±3	140 ² , 139 ³ , 155 ⁴
NaNO_2	110±3	119 ² , 114 ⁵ , 117 ⁷ , 100 ⁸
KNO_3	142±5	140 ² , 142 ³ , 141 ⁷ , 138 ⁹ , 130 ¹⁰ , 141 ¹¹
HTS_1	126±2	131 ⁶ , 132 ¹⁰
HTS_2	139±2	136 ¹² , 142 ¹³ , 155 ¹⁴

Table V
Heat capacity of liquid phase in binary and ternary systems

Composition, mol%			Liquidus temp., K	$C_p(l)$, J/K/mol
NaNO_3	NaNO_2	KNO_3		
20.00	80.00	0.00	520	118±4
40.00	60.00	0.00	500	122±4
60.00	40.00	0.00	519	125±8
80.00	20.00	0.00	549	129±4
0.00	20.00	80.00	531	134±3
0.00	40.00	60.00	420	128±2
0.00	60.00	40.00	410	119±2
0.00	80.00	20.00	487	113±2
80.00	0.00	20.00	542	134±5
60.00	0.00	40.00	504	134±5
50.00	0.00	50.00	495	139±2
40.00	0.00	60.00	497	138±2
20.00	0.00	80.00	555	136±5
20.00	42.00	38.00	429	120±2
40.00	31.50	28.50	455	128±8
60.00	21.00	19.00	502	127±5
80.00	10.50	9.50	545	131±2

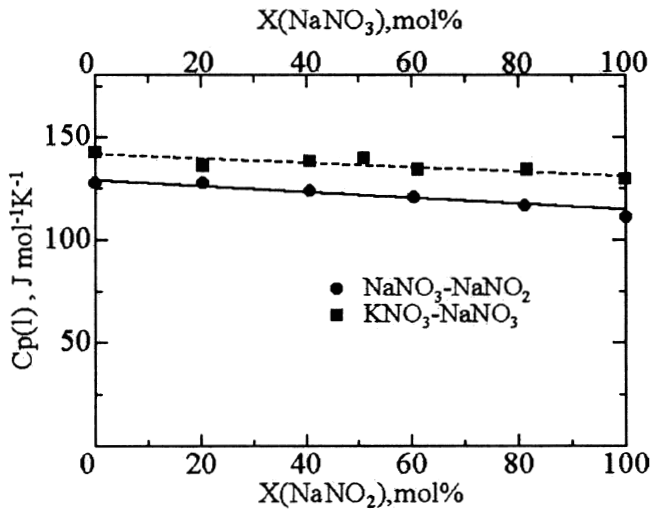


Figure 9. Heat capacity of liquid $\text{NaNO}_3\text{-NaNO}_2$ and $\text{KNO}_3\text{-NaNO}_3$ systems

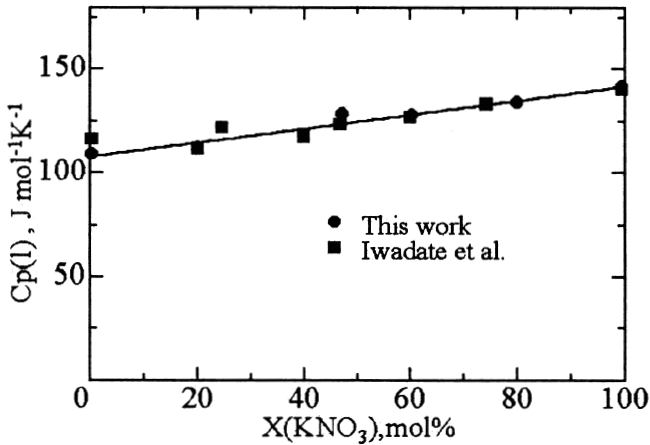


Figure 10. Heat capacity of liquid $\text{NaNO}_2\text{-KNO}_3$ system

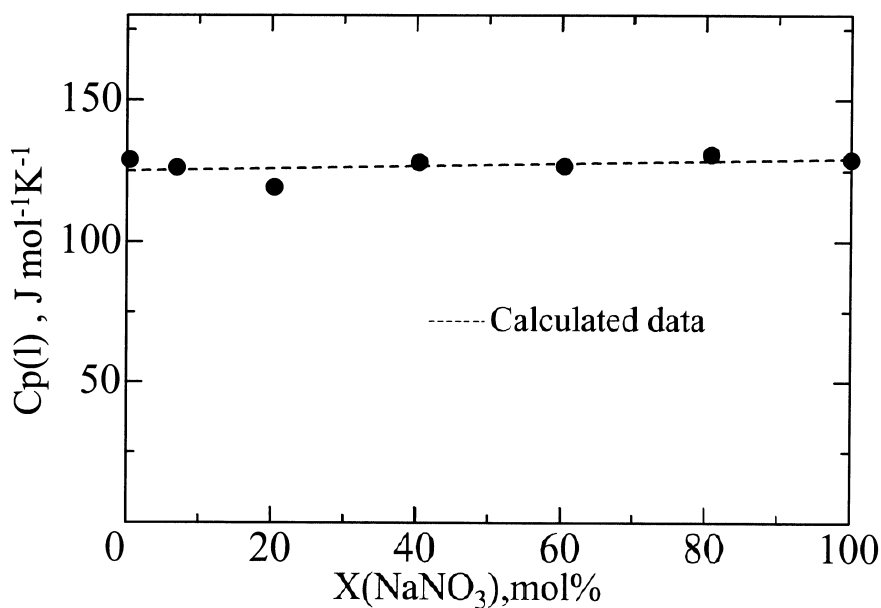


Figure 11. Heat capacity of liquid $\text{NaNO}_3\text{-NaNO}_2\text{-KNO}_3$

Figure 11 shows the change of heat capacity with NaNO_3 content in the $\text{NaNO}_3\text{-NaNO}_2\text{-KNO}_3$ ternary system along the line passing the composition of HTS_1 as shown in Figure 1. The broken line shows the sum of the heat capacities of the constituent elements. Therefore, Neumann-Kopp's law can also be seen in this ternary system.

Estimation of heat loss during the experiment

Experiment with liquid phase salt

The heat will be lost during pouring of liquid salt from the Tammann tube trough the hole to the calorimeter. One is the convective heat loss and the other is the radiative heat loss. The former is estimated as follows. The amount of convective heat loss is given by

$$Q_{con.} = \int_0^{t_f} \alpha A \Delta T dt \quad [10]$$

where, t_f is the dropping time of salt, α is the heat transfer coefficient between the falling salt column and ambient air, A is the surface area of the falling column, and ΔT is the temperature difference between the falling salt and ambient air. Assuming the parallel flow of air along the falling column, the heat transfer coefficient is given by

$$Nu = \frac{\alpha d}{\lambda} = 0.56cRe^m Pr^{0.31} \quad [11]$$

where, Nu is the Nusselt number, d is the diameter of the column, λ is the thermal conductivity of air, Re is the Reynolds number, Pr is the Prandtl number, and c and m are coefficients depending on the range of Re . In the case where the molten salt of 600 K passed through the ambient air of 298 K, using the following data of $v=0.312 \times 10^{-4} \text{ m}^2/\text{s}$, $\lambda=0.034 \text{ J/m/s/K}$, $Pr=0.71$ for air at the average temperature of molten salt and ambient air¹⁶ and $d=0.004 \text{ m}$, $A=0.0005 \text{ m}^2$, $u=0.44 \text{ m/s}$, $t_f=3 \text{ s}$ for falling salt column, the Re was calculated as 56.4. Then, $c=0.615$ and $m=0.466$ were obtained from the literature¹⁶. Then, the Nu was calculated as 8.14 and α was $0.070 \text{ kJ/m}^2/\text{s/K}$. Finally, the convective heat loss, $Q_{con.}$ was estimated as 0.003 kJ .

The latter is estimated by the following Equation.

$$Q_{rad.} = \int_0^{t_f} \epsilon \sigma F T^4 dt \quad [12]$$

where, σ is the Stefan-Boltzmann constant, 5.68×10^{-11} kJ/m²/s/K⁴, ϵ is the emissivity. The emissivity data of the present molten salt was not found. Therefore, the data of water which is the largest among liquids was used, namely, $\epsilon=0.95^{16}$. Then the radiative heat loss, $Q_{rad.}$ was estimated as 0.010 kJ.

The total heat loss was estimated as 0.013 kJ. Since the heat absorbed by the calorimeter Q_c was approximately 7kJ, the error due to the heat loss during dropping was estimated as 0.2 per cent.

Determination of water equivalent

The convective heat loss is also estimated by Equation [10] also in this case. However, the relative flow condition was different from the falling salt column but perpendicular to the flow against the copper piece. In this case, the coefficients c in Equation [11] is 1.11. In the case where the copper piece of 373 K was dropped through the ambient air of 298 K, the data of $\nu=0.196 \times 10^{-4}$ m²/s, $\lambda=0.029$ J/m/s/K, $Pr=0.71$ for air at the average temperature of the copper piece and ambient air. Using the data of $d=0.015$ m, $A=0.002$ m², $u=0.1$ m/s and $t_f=3$ s, the convective heat loss, $Q_{con.}$ was estimated as 0.006 kJ. The radiative heat loss was estimated by Equation [12]. The emissivity of copper was taken from the literature as 0.052. Then the radiative heat loss, $Q_{rad.}$ was estimated as 0.001 kJ. The total heat loss was estimated as 0.007 kJ. Since the heat absorbed by the calorimeter Q_c was approximately 3.5 kJ, the error due to the heat loss during dropping was estimated as 0.2 per cent.

Experiment with solid phase salt

The temperature difference between the solid salt sample and the ambient air was so small that any heat loss was not taken into account.

Conclusion

- A simplified drop calorimetric method was proposed to measure the heat capacity of molten salt mixtures.
- The standard enthalpy of molten NaNO₃-NaNO₂-KNO₃ mixture and heat of dissolution of the salts into water was obtained.
- The heat capacity of pure NaNO₃, NaNO₂ and KNO₃ was 0.129 ± 0.003 , 0.110 ± 0.003 and 0.142 ± 0.005 kJ/mol/K, respectively. These data are in good agreement with the literature data.

- The heat capacity of HTS₁ was 0.126 ± 0.002 kJ/K/mol which was slightly smaller than the literature data. That of HTS₂ was 0.139 ± 0.002 kJ/K/mol which was in the middle of the literature data.
- Neumann-Kopp's law was confirmed for the molten salt mixture of the present composition.

References

1. KIRST, W.E., NAGLE, W.M., and CASTNER, J.B. *Trans. Am. Inst. Chem. Engr.* vol. 36 1979, pp. 371–394.
2. CARLING, R.W. *Thermochemica Acta*, vol. 60 1983, pp. 265–275.
3. ICHIKAWA, K. and MATSUMOTO, T. *Bull. Chem. Soc. Jpn*, vol. 56 1983, pp. 2093–2100.
4. DWORKIN, A.S. and BREDIG, M.A. *J. Phys. Chem.*, vol. 67 1963, p. 697.
5. Kamimoto, M. *Thermochemica Acta*, vol. 41 1980, pp. 361–369.
6. JANZ, G.J. and TRUONG, G.N. *J. Chem. Eng. Data*, vol. 28 1983, pp. 201–202.
7. IWADATE, Y., OKADA, I., and KAWAMURA, K. *J. Chem. Eng. Data*, vol. 27 1981, pp. 288–290.
8. CASES, J.C. *Revue De Chimie Minerale*, vol. 10 1973 pp. 577–583.
9. CLARK, R.P. *J. Chem. Eng. Data*, vol. 18 1973, pp. 67–70.
10. DAGLAS, T.B. *Trans. ASME*, vol. 79 1957, p. 23.
11. GOODWIN, H.M. and KALMUS, T.H. *Phys. Rev.*, vol. 28 1909, p. 1.
12. KAMIMOTO, M. *Thermochemica Acta*, vol. 49 1981, pp. 319–331.
13. NGUYEN-DUY, P. and DANCY, E.A. *Thermochemica Acta*, vol. 39 1980, p. 95.
14. VOSKRESENSKAYA, N.K., YANKOVSKAYA, G.N., and ANOSOV, V.Y. *Zh. Prikl. Khim.* vol. 21 1948, pp. 18–25
15. *Kagaku-binnran* (in Japanese), ed. by Japan Chemical Society, 1975 pp. 924–25.
16. *Kikaikougaku-binnrann* (in Japanese), ed. by the Japan Society of Mechanical Engineers, vol. 2 1976, p. 10.

